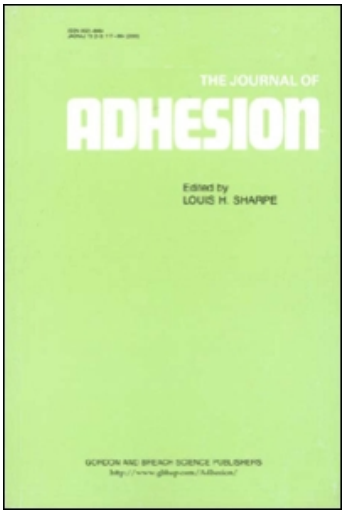

The Journal of Adhesion
Publication details, including instructions for authors and subscription information:
http://www.informaworld.com/smpp/title~content=t713453635

Influence of Residual Thermal Stresses on the Fracture Behavior of Hybrid Bonded Joints

H. Orsini[a]; F. Schmit[a]
[a] D.G.A./Centre de Recherches et d'Etudes d'Arcueil, Arcueil, France

To cite this Article Orsini, H. and Schmit, F.(1993) 'Influence of Residual Thermal Stresses on the Fracture Behavior of Hybrid Bonded Joints', The Journal of Adhesion, 43: 1, 55 — 68
To link to this Article: DOI: 10.1080/00218469308026587
URL: http://dx.doi.org/10.1080/00218469308026587

J. Adhesion, 1993, Vol. 43, pp. 55–68
Reprints available directly from the publisher
Photocopying permitted by license only

Printed in the United States of America

Influence of Residual Thermal Stresses on the Fracture Behavior of Hybrid Bonded Joints

H. ORSINI and F. SCHMIT

D.G.A./Centre de Recherches et d'Etudes d'Arcueil, 94114 Arcueil, France

(Received September 30, 1992; in final form May 26, 1993)

The objective of this work is to study the influence of the residual thermal stresses on the fracture behavior of hybrid composite-aluminium bonded joints. A modified DCLS specimen is designed and the strain energy release rate is determined using both an analytical fracture mechanics based method and a finite element method. The residual thermal stresses, which appear in the adhesive because of the difference between the curing and the service temperatures, are evaluated with a two-ply laminate specimen. Some rupture tests are performed on the DCLS specimens at different temperatures and for different geometries and materials. The results show a good agreement between analytical calculations, numerical analysis and experiments. The residual thermal stresses are never negligible in the considered hybrid bonded joints and do influence their fracture behaviors. Although the designed specimen is not adapted to study fatigue crack propagation, it provides a simple way to study the crack initiation and thus to characterize the rupture properties of the joint.

KEY WORDS adhesive bonding; composite/aluminium joint; finite element analysis; fracture mechanics; mixed mode loading; crack propagation; theory; experiment; thermal stresses; numerical analysis; double crack lap shear specimen.

1. INTRODUCTION

Bonding techniques are used in an ever-growing number of applications: electronics (multilayer boards, bonded components), aerospace and aeronautical industries (F-18 bonded wings), car industries and many more. Joining structural components with adhesives offers many advantages over conventional mechanical fasteners: lower structural weight, lower fabrication cost, and improved damage tolerance have been demonstrated.[1-4] Adhesives can also be used to join layers of different materials to make one new improved material. For example, hybrid bonded systems of metal and composite layers are stronger for equal weight and stiffness than metals alone.[5] Even with all the advantages and encouraging experiences with adhesive bonding, manufacturers still hesitate to apply this technology to primary structural components, citing a lack of confidence from poor understanding. There is, therefore, a growing need to assess the rupture performance of bonded joints.

Mostovoy and Brussat[6] have proposed to use fracture mechanics theory to design adhesive joints. Such an approach presents some advantages compared with the classical method: it is conservative, since the damage is taken into account, and it can deal with cyclic loading and creep. However, it requires the study of different types of loading: mode I, mode II and mixed mode I+II. Many articles can be found in the literature on the design and the uses of different specimens, on experiments and on the determination of fracture laws. The geometry of the test specimens must fulfil two main requirements: it must be simple enough to be numerically or analytically modelled and it must represent the joint configuration in service.

Fewer studies have been carried out on the bonding of dissimilar materials.[7] If the materials have different thermal expansion coefficients, residual stresses appear in the adhesive due to the difference between the curing temperature and the service temperature. In some cases, the induced stresses can be important and can modify the mechanical performance of the bonded structure.

The aims of this work are to design a specimen to study the static and fatigue fracture of hybrid bonded joints, to model this specimen and then to characterize an aluminium-composite bonded joint, taking into account the thermal phenomena. The first part presents the geometry and characteristics of the specimen chosen. Then, the strain energy release rate is numerically and analytically determined. Finally, some fracture experiments are carried out to correlate the analytical and numerical results.

This study is a part of an English–French collaboration between DGA/Centre de Recherches et d'Etudes d'Arcueil (F) and DRA/Royal Aerospace Establishment (GB) on bonded joints.

2. SPECIMEN DESIGN AND FABRICATION

Figure 1 shows the two basic joint configurations chosen for the present analysis. The first one, named CAC, consists of an aluminium strap and two carbon-epoxy unidirectional composite lap adherends bonded to each side of the aluminium. The second one, named ACA, consists of a carbon-epoxy unidirectional composite strap and two aluminium lap adherends bonded to each side of the composite. Both specimens are designed so that the product of thickness by Young's modulus of each material system remains constant. Both materials are assembled with EA 9628 NW adhesive film supplied by Dexter Corporation, Hysol Division. It is a modified epoxy resin known for its good toughness. The specimens are cut out from panels obtained by autoclave bonding the three plates following the conditions recom-

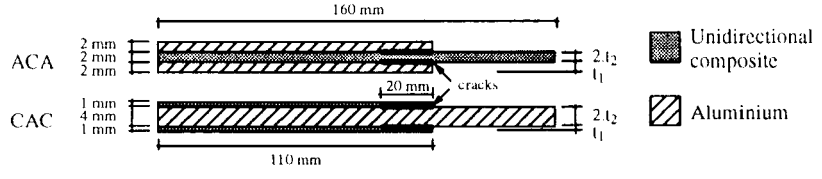

FIGURE 1 Joint configurations.

TABLE I
Properties of materials

7075T6 aluminium alloy:	$E = 71$ GPa	
	$\nu = 0.33$	
	$\alpha = 23.5 \times 10^{-6}$ K^{-1}	
HYSOL EA 9628 adhesive:	$E = 2.2$ GPa	
	$\nu = 0.38$	
	$\alpha = 45 \times 10^{-6}$ K^{-1}	
T300/5245C unidirectional composite:	E_1	$= 142$ GPa
	$E_2 = E3$	$= 9.9$ GPa
	$\nu_{12} = \nu_{13}$	$= 0.29$
	$\nu_{21} = \nu_{31}$	$= 0.02$
	$\nu_{23} = \nu_{32}$	$= 0.5$
	α_1	$= 0$ K^{-1}
	$\alpha_2 = \alpha_3$	$= 30 \times 10^{-6}$ K^{-1}
T800/5245C unidirectional composite:	E_1	$= 174$ GPa
	$E_2 = E_3$	$= 9.64$ GPa
	$\nu_{12} = \nu_{13}$	$= 0.36$
	$\nu_{21} = \nu_{31}$	$= 0.02$
	$\nu_{23} = \nu_{32}$	$= 0.5$
	α_1	$= 0$ K^{-1}
	$\alpha_2 = \alpha_3$	$= 30 \times 10^{-6}$ K^{-1}

mended by the supplier (90 minutes at 120°C under 2 bars pressure). The two cracks are created during the curing process with Mylar® films. Material properties are detailed in Table I.

These modified Double Crack Lap Shear (DCLS) specimens were chosen for this study because they represent a typical mixed-mode loading of large bonded areas of many structural applications. Moreover, since they are symmetric, the non-linear geometric effects can be avoided and the specimens can be treated as geometric linear structures. These specimens are, therefore, well designed to study the fracture behavior of the bonding of dissimilar materials.

3. CALCULATION OF STRAIN ENERGY RELEASE RATE

3.1 Analytical Determination of G

The chosen parameter for this study is the strain energy release rate, G. It is defined as:

$$G = \frac{1}{w}\left(\frac{dW}{da}\right) - \frac{dU}{da}$$

where w is the specimen width, W is the work done by the applied load and U is the stored strain energy. When fracture occurs, $G = G_c$, the critical strain energy release rate. G depends on the specimen geometry and materials. For the considered system, G_c is a characteristic of the adhesive, provided that the rupture occurs in a cohesive way.

G is a suitable parameter since, in bonded joints, the irreversible dissipations are usually located in a small zone around the crack tip and confined between two elastic

substrates. This corresponds to the small scale yielding conditions where linear elastic fracture mechanics is valid. For this particular bonded structure the strain energy release rate has been determined by Roderick *et al.*[8] under thermo-mechanical loadings using simple beam theory. The calculations are made with the following assumptions:

—the substrates are linear elastic and loaded in pure tension (rigid in bending)
—the bonded joint is assumed to be perfect

G can then be expressed as:

$$G = \frac{t_1 \cdot t_2 \cdot E_1}{E_2 \cdot (t_1 \cdot E_1 + t_2 \cdot E_2)} [S - \Delta T(\alpha_1 - \alpha_2) \cdot E_2]^2 \tag{1}$$

S is the stress applied to the strap adherend. t_1 and E_1 are, respectively, the thickness and the Young's modulus of a lap adherend. t_2 and E_2 are, respectively, the half-thickness and the Young's modulus of the strap adherend. α_1 and α_2 are the coefficients of thermal expansion. ΔT is the change of temperature from the "stress-free temperature." The "stress-free temperature" is usually the smaller of the glass transition temperature and the curing temperature. In our case, the "stress-free" temperature corresponds to the curing temperature.

3.2 Numerical Determination of G

The specimens were meshed on the finite element code ABAQUS. Four-node plane stress elements were used. Only half of the specimens were meshed because of the symmetry. Figure 2 shows a typical mesh with the symmetry, the loading and the limit conditions. G was computed with two methods:

J-integral First introduced by Rice,[12] the J-integral can be used as a non-linear fracture mechanics parameter for an elastic problem. J is shown to be equivalent to the strain energy release rate, G, in linear elastic cases. The finite element code ABAQUS directly computes this parameter.

Crack closure technique The crack closure technique is widely described in the literature.[9–11] The contention is that if a crack extends by a small amount, the strain energy released in the process is equal to the work required to close the crack to its original length. This method has the advantage of giving G_I and G_{II} in a single analysis: G_I is calculated from the force and displacement components normal to the rotated bond line and G_{II} is obtained from the corresponding tangential components. Referring to Figure 3, G_I and G_{II} are given by:

$$\begin{cases} G_I = \lim\limits_{\Delta c \to 0} \dfrac{1}{2\Delta c} F_c(v_c - v_d) \\ \\ G_{II} = \lim\limits_{\Delta c \to 0} \dfrac{1}{2\Delta c} T_c(u_c - u_d) \end{cases} \quad \text{and} \quad G = G_I + G_{II} \tag{2}$$

The value of F_c and T_c are taken to be the y- and x-forces, respectively, that are required to hold nodes c and d together. u_c, v_c, u_d and v_d are the displacements of the nodes c and d. Δc is the crack extension. F_c, T_c, u_c, v_c, u_d and v_d are given by the finite element analysis.

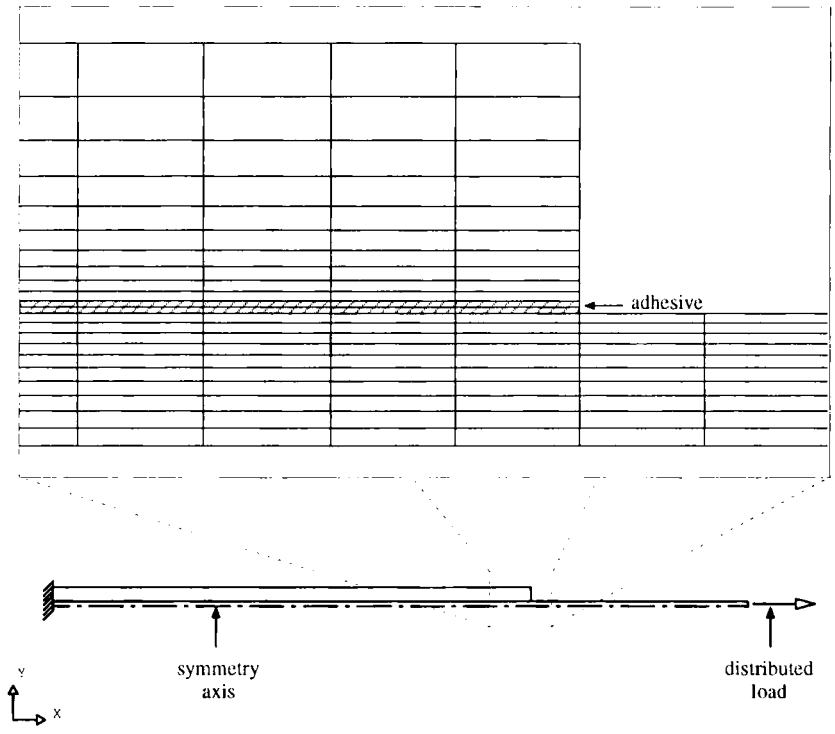

FIGURE 2 Typical Mesh (ACA specimen).

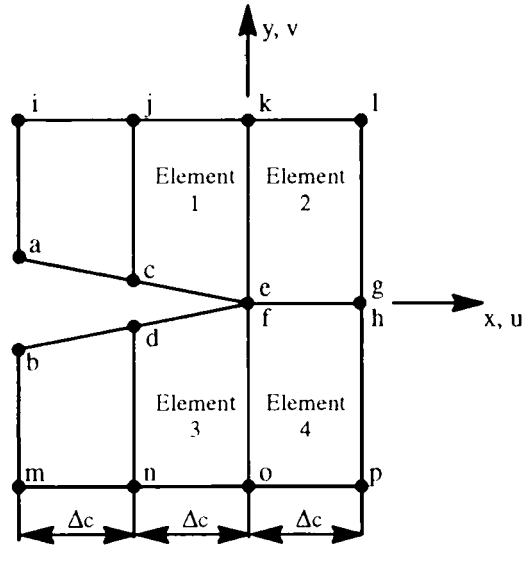

FIGURE 3 Finite element nodes near crack tip.

3.3 Results

The following stresses have been applied to the specimens: mechanical (tension up to 500 MPa), thermal (ΔT = room temperature − curing temperature = 20°C − 120°C = − 100°C) and thermo-mechanical which takes the residual thermal stresses into account (tension up to 500 MPa and $\Delta T = -100°C$). A comparison is first made between the different methods of computing G, and then the influence of the following parameters on G and on the ratio G_I/G_{II} is studied for the three loadings:

—crack length (20 to 90 mm)
—adhesive joint thickness (0 to 0.8 mm)
—Young's modulus of the adhesive (0 to 10 GPa)
—crack position in the joint thickness planes

The computations were made for different element sizes in order to study the mesh-dependence of the finite element analysis. No significant difference appeared in the

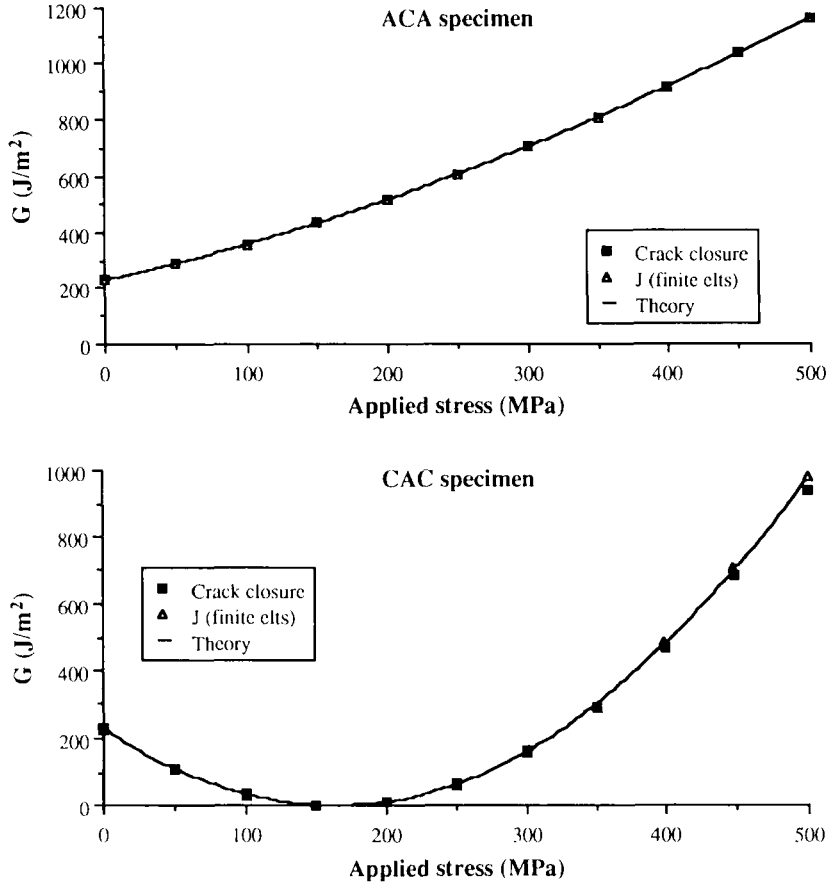

FIGURE 4 Computation of G (thermo-mechanical loading).

results. This allowed the use of a relatively large size of elements (1 mm^2 for the substrates around the crack zone).

Figure 4 presents the comparison of the three calculations of G for a thermo-mechanical loading. It can be seen that the three methods of computing G are in very good agreement (for the ACA specimen, the symbols representing the crack closure method and the finite element computation are superimposed on the figure). In Figure 5, G_{mech} is computed considering a mechanical loading only, and G_{tm} is computed considering a thermo-mechanical loading. This graph highlights the considerable influence of the residual thermal stresses on the value of G. Even when the applied stress is high, the effect of the residual thermal stresses is not negligible.

Considering the particular case of the ACA specimen with an adhesive thickness of 0.05 mm, no effect of the crack length on G is noticed, as shown in Figure 6. This specimen should thus allow the study of the crack growth phases (*e.g.* for fatigue loading). The G_I/G_{II} ratio is about 0.35 for the chosen adhesive and thickness, and is independent of the crack length.

The adhesive thickness, the Young's modulus of the adhesive and the position

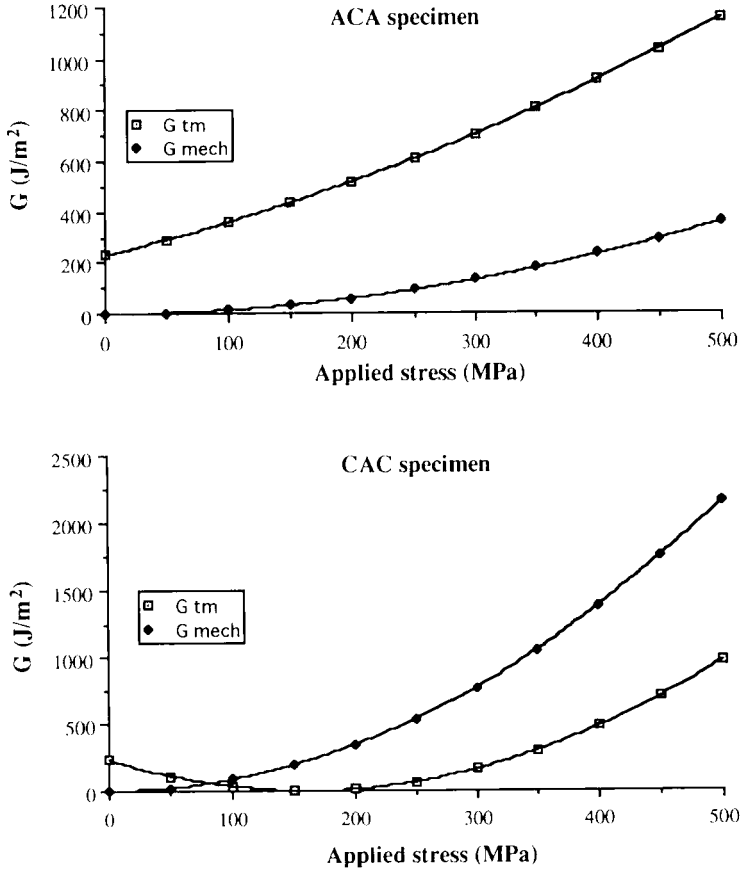

FIGURE 5 Influence of thermal stresses on G.

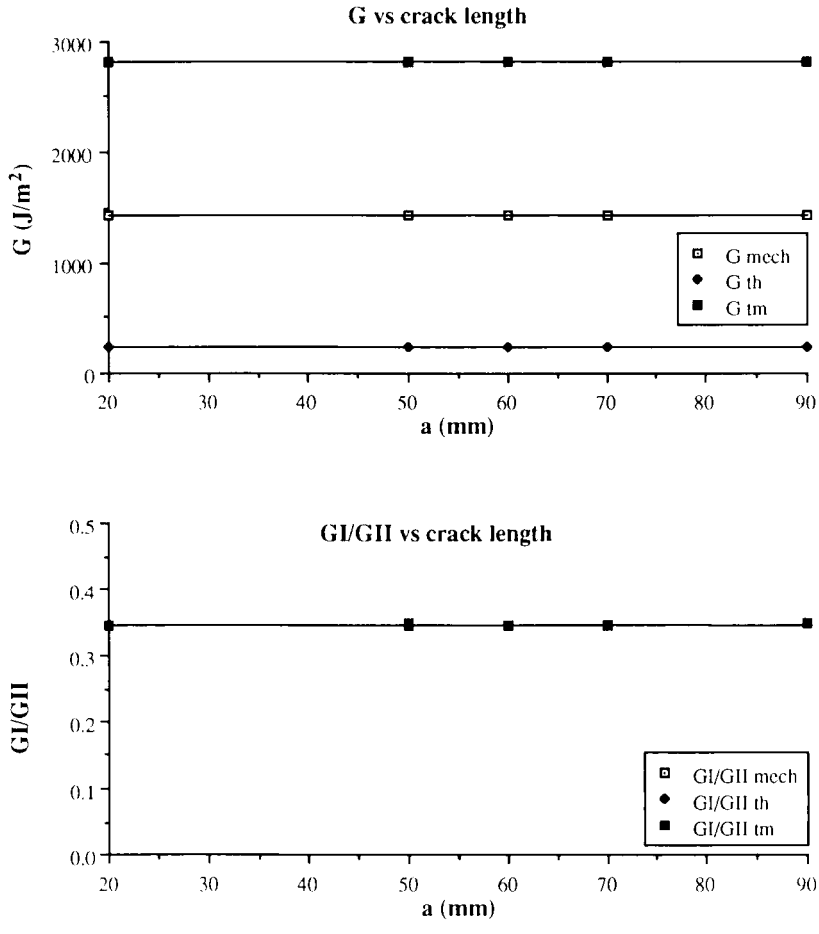

FIGURE 6 Influence of crack length (a) on G and G_I/G_{II}. ACA specimen, 0.05 mm thick joint.

of the crack in the joint have no effect on G (graph not shown). It can be seen in Figure 7 that the G_I/G_{II} ratio is strongly dependent on the joint characteristics. However, since the crack tip is the scene of complex phenomena of plasticity and damage, these effects cannot be given too much importance.

3.4 Effect of Asymmetric Cracks

The case where the crack lengths are different has been briefly studied. Non-linear effects have been taken into account in the finite element analysis. It appears that the longer crack has the higher G until the difference between the crack lengths reaches a critical value which depends on the loading. Though this phenomenon has not been observed in the fracture experiments described in Section 4.2, it could occur in the case of fatigue tests and provoke asymmetric crack growths.

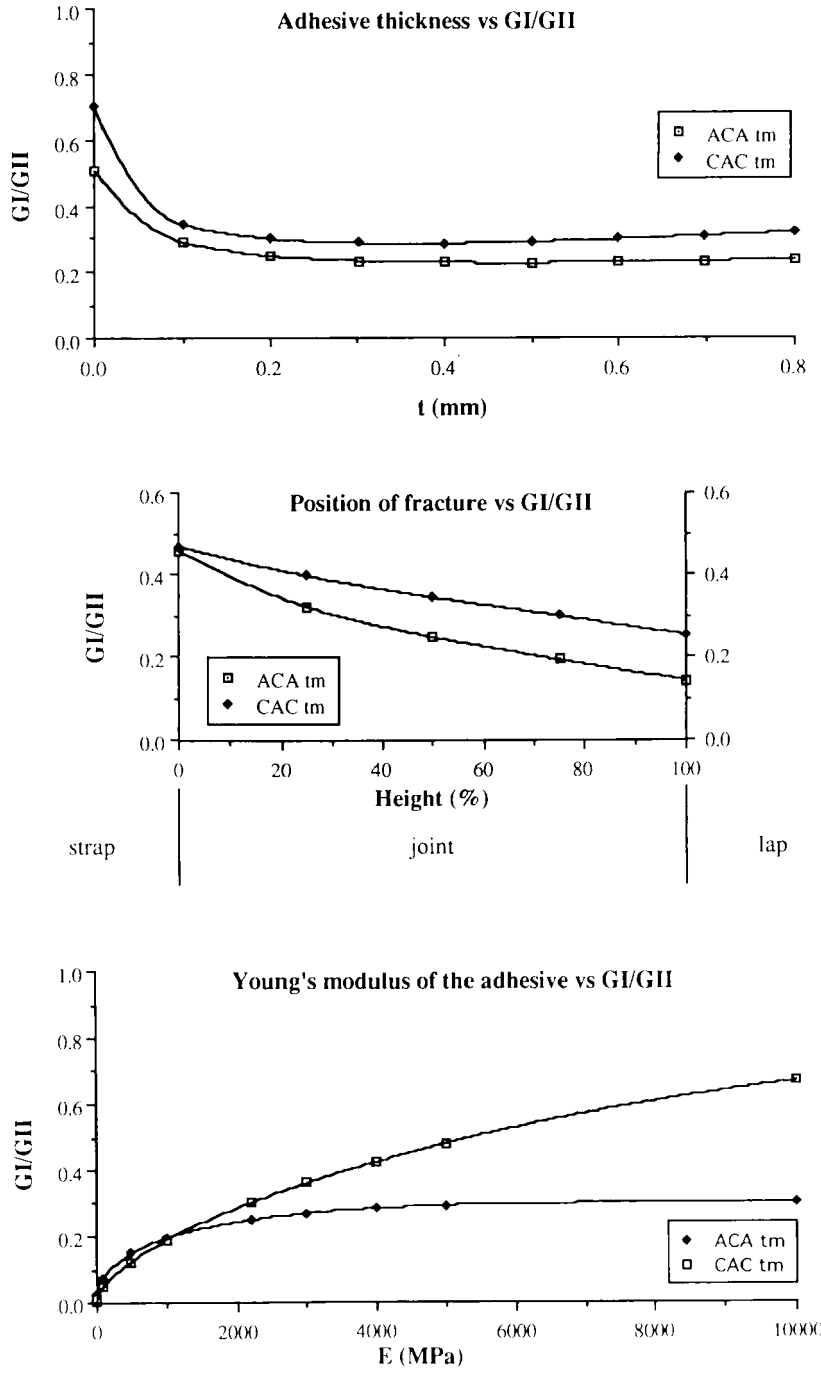

FIGURE 7 Influence of the adhesive characteristics on G_I/G_{II}.

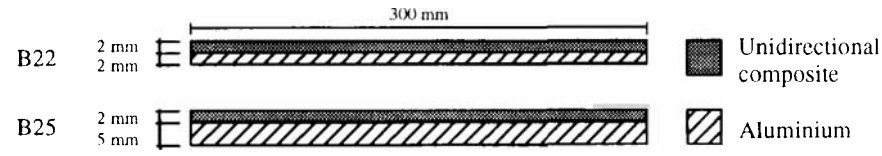

FIGURE 8 Laminates used to evaluate the residual thermal stresses.

4. FRACTURE EXPERIMENTS AND DISCUSSION

4.1 Evaluation of Thermal Stresses

The experimental evaluation of the thermal stresses ($E \cdot \Delta\alpha \cdot \Delta T$) are carried out using the two-ply laminate method. This method consists of measuring the deflection of a laminate made of a carbon-epoxy and an aluminium plate bonded together with the Hysol EA 9628 NW adhesive. The specimens used, named B22 and B25, are shown in Figure 8 and the materials are described in Table I. The curing process is the same as for the ACA and CAC specimens (see Section 2).

Assuming both plates of the laminate are perfectly bonded, beam theory gives:[13]

$$\Delta\alpha \cdot \Delta T = \frac{t_1 + t_2}{2\rho} + \frac{(t_1^3 E_1 + t_2^3 E_2)\left(\frac{1}{t_1 E_1} + \frac{1}{t_2 E_2}\right)}{6\rho\,(t_1 + t_2)} \quad \text{where } \rho = \frac{4h^2 + l^2}{8h} \tag{3}$$

E and t are, respectively, the Young's modulus and the thickness of each material. ρ is the radius of curvature and h is the deflection of the laminate. l is the specimen length and is assumed to be independent of temperature.

It is, therefore, possible to evaluate the residual thermal stresses. The deflection at room temperature has been experimentally measured with a LVDT transducer and computed by finite element analysis assuming the bonded joint is perfect, in order to evaluate the influence of the adhesive layer. This deflection corresponds to a thermal loading: ΔT = room temperature − "stress-free" temperature = room temperature − curing temperature = −100°C. The results are compared in Table II and they exhibit good agreement. It is thus valid not to take the adhesive layer into account.

The evolution of the deflection with temperature has also been measured.The laminate was placed in a temperature-controlled chamber, the deflection variation was measured with a LVDT transducer, and the temperature with a thermocouple.

TABLE II
Measure of the deflection of the laminates at room temperature

	Experiment (mm)	Finite element analysis (mm)
B22	5.1	5.3
B25	2.9	3.0

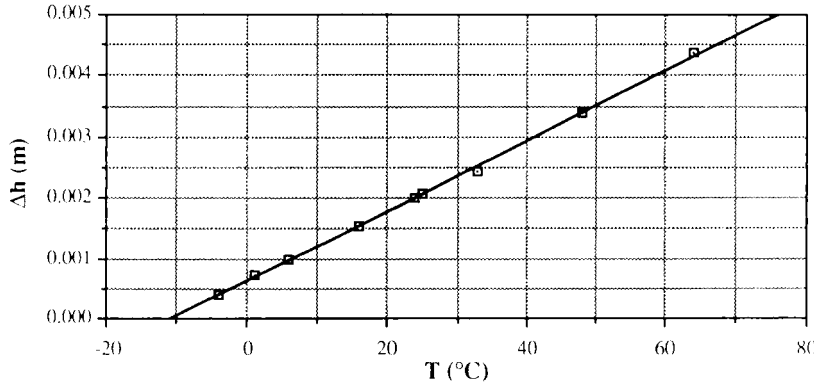

FIGURE 9 Deflection *versus* temperature (laminate specimen B22).

This experiment was repeated for several specimens. One of the curves is presented in Figure 9, the others being similar. The slope of the deflection variation *versus* temperature curve can easily be related to $\Delta\alpha$ through a first order limited development of equation 3, considering the deflection variation is infinitesimally small compared with the specimen length. The experimental $\Delta\alpha$ is 25×10^{-6}, and material data give $\Delta\alpha = 23 \times 10^{-6}$.

4.2 Fracture Tests

Experimental process The rupture specimens ACA and CAC are presented in Figure 10. They are loaded in tension, as shown in Figure 11, with a mechanical Instron testing machine equipped with a 100 kN loading cell and a temperature-controlled chamber. The computation of the critical strain energy release rate, G_c, requires the determination of the load at which the crack occurs. This is done with acoustic emission following a method described by Ziane and Coddet.[14] The load-displacement curve is recorded along with the acoustic event cumulative curve. A schema of a typical experimental record is given in Figure 12. Before the adhesive cracks, the event cumulative curve shows a low slope corresponding to microscopic

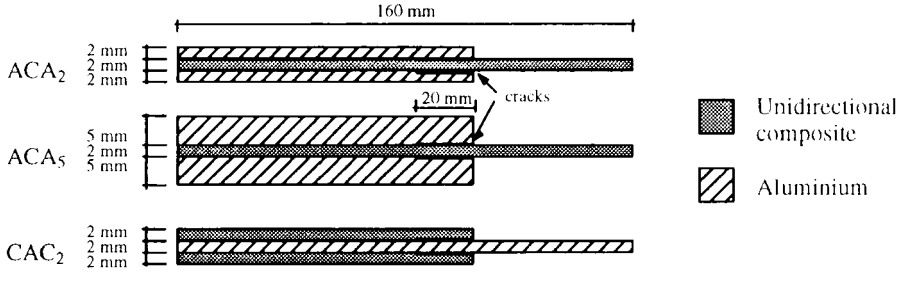

FIGURE 10 Rupture specimens.

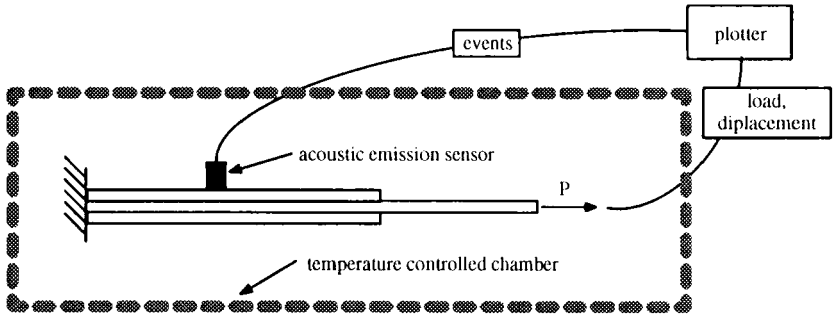

FIGURE 11 Rupture test configuration.

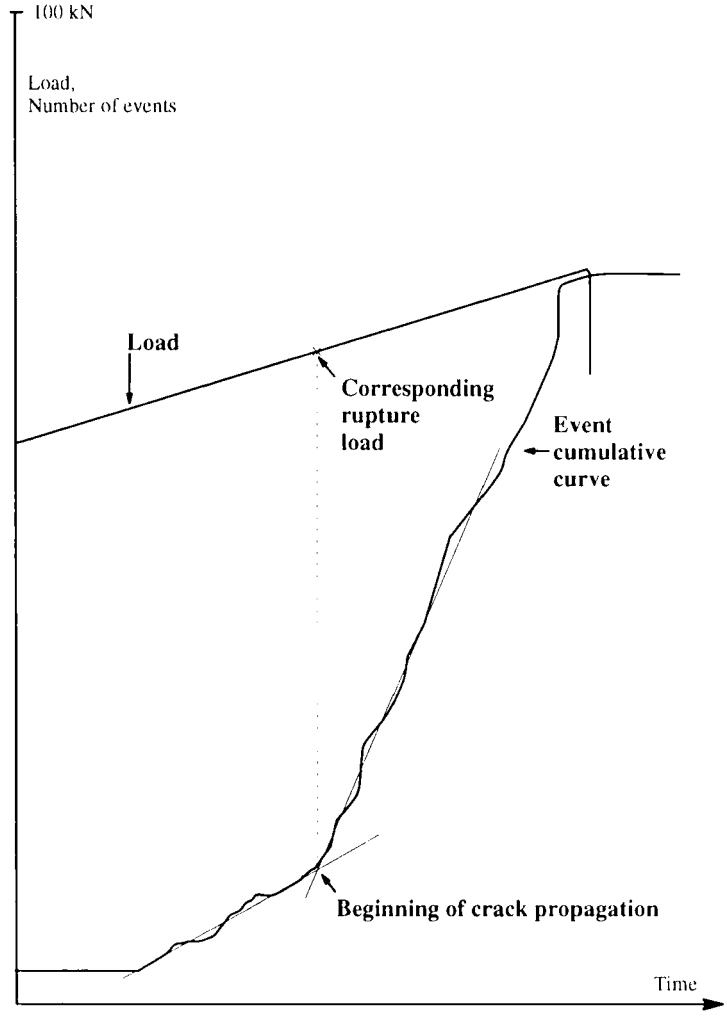

FIGURE 12 Acoustic emission record during a fracture test.

TABLE III
Results of the rupture tests

	Temperature (°C)	Load (kN)	G_{mech} (kJ/m^2)	G_{tm} (kJ/m^2)
ACA_2 T300	20	62 (3.1)	2.7 (0.35)	4.3 (0.35)
ACA_2 T800	20	72 (9.1)	2.6 (0.85)	4.4 (0.85)
ACA_5 T800	20	51 (1.0)	2.0 (0.11)	3.9 (0.11)
ACA_2 T800	−10	70 (1 test)	2.5 (1 test)	4.8 (1 test)
ACA_5 T800	−10	48 (1 test)	1.7 (1 test)	4.2 (1 test)

damage. When rupture occurs, the slope of the cumulative curve becomes higher and marks the propagation of the crack. The load corresponding to the change in slope is taken to be the one at which the crack begins to propagate. G_c is then computed using eq. 1. In order to verify that G_c is an intrinsic characteristic of the adhesive, two composites and two geometries were tested. A few experiments were performed at a temperature of −10°C; they did not provide an accurate result, but give an order of magnitude.

Results The CAC specimens fractured in the aluminium strap. They are, therefore, not adapted to the experiment which focused on the ACA specimens.

The results are given in Table III. G_{mech} is computed considering a mechanical loading only, whereas the residual thermal stresses are taken into account for G_{tm}. When several experiments were carried out for the same configuration, the figure given is the mean and the standard deviation, σ_{n-1}, is shown in brackets.

4.3 Discussion

For the ACA specimens, the fracture first occurs in a cohesive way, then becomes adhesive along the composite-adhesive interface and finally propagates in the composite. Therefore, G_c is an intrinsic characteristic of the adhesive and should be constant.

The results presented in Table III exhibit an important difference between G_{mech} and G_{tm}. However, only the consideration of thermal stresses allows a rationalization of the results and gives a constant critical strain energy release rate: $G_c \approx 4.2$ kJ/m^2.

The rupture of the CAC specimens in the aluminium strap can then easily be explained. Indeed, the rupture occurs in the substrate if:

$$G_c > \frac{t_1 t_2 E_1}{E_2(t_1 E_1 + t_2 E_2)} [S_r - \Delta T(\alpha_1 - \alpha_2)E_2]^2$$

where S_r is the rupture strength of the strap adherend. Considering the CAC specimens, this criterion becomes: $G_c > 2.9$ kJ/m^2. It is verified only if the residual thermal stresses are taken into account in the computation of G_c.

5. CONCLUSION

This work has shown that the thermal stresses in unidirectional composite-aluminium bonded joints are very important and never negligible. They can be taken into account by using a Fracture Mechanics based approach. A very good agreement between analytical calculations, numerical analysis and experiments has been found.

The DCLS specimen used presents some disadvantages for the study of hybrid bonded joints: it has been shown that a non-symmetrical propagation of the cracks is favoured. It is, therefore, not adapted to the study of fatigue crack propagation. However, it represents a typical mixed-mode loading and, since it is symmetric, it can be treated as a geometrically-linear structure. Therefore, it provides a simple way to study the crack initiation and thus to characterize the rupture properties of the joint. Moreover, a particular mode distribution can be obtained by adjusting the specimen geometry and materials. This allows the establishment of a part of the rupture envelope. This specimen could also be used in a simple and cost-effective quality control test during the fabrication of a bonded structure.

Acknowledgments

The financial support of DGA/DRET/Service Des Recherches has been greatly appreciated.

References

1. D. L. Potter *et al.*, "Primary Adhesively Bonded Structure Technology (PABST), Design Handbook for Adhesive Bonding," AFFDL-TR-79-3129, Nov. 1979.
2. J. L. Maris and G. E. Kuhn, "Advanced Technology Wing Structure," AFWAL-TR-80-3031, May 1980.
3. T. J. Reinhart, "Future Applications of Adhesive Bonding in the U.S. Air Force," SAMPE, *The Science of Advanced Materials and Process Engineering Series* **26,** 642–651 (1981).
4. R. R. Irving, "A Tale of Adhesively Bonded Aircraft," *Iron Age*, p. 87–88, May 4, 1981.
5. R. W. Johnson and R. R. June, "Application Study of Filamentary Composites in a Commercial Jet Aircraft Fuselage," NASA CR-112110, 1972.
6. T. R. Brussat, S. T. Chiu and S. Mostovoy, "Fracture Mechanics for Structural Adhesive Bonds—Final report" AFML-TR-77-163, 1977.
7. F. Roudolff, *La Recherche Aérospatiale* No. 1, 49–55 (1990).
8. G. L. Roderick, R. A. Everett, Jr. and J. H. Crews, Jr., "Cyclic Debonding of Unidirectional Composite Bonded to Aluminium Sheet for Constant-Amplitude Loading," NASA TN D-8126.
9. E. F. Rybicki and M. F. Kanninen, *Engineering Fracture Mechanics* **9,** 931–938 (1977).
10. C. J. Jih and C. T. Sun, *Engineering Fracture Mechanics* **37,** 313–322 (1990).
11. B. Dattaguru, R. A. Everett, Jr., J. D. Whitcomb and W. S. Johnson, *J. Eng. Mater. and Technol.* **106,** 59–65 (1984).
12. J. R. Rice, *J. Appl. Mechanics, Transactions of the ASME* **379,** 376–386 (1968).
13. R. Prépin, C. Cazeneuve and G. Pluvinage, *Compte-Rendu des 6èmes Journées Nationales sur les Composites*, p. 343–352, 1988.
14. E. Ziane and C. Coddet, *Adhesively Bonded Joints: Testing, Analysis and Design*, **ASTM STP 981** 183–193 (1983).